Solvent-free lithium and sodium containing electrolytes based on pseudo-delocalized anions

ChemComm

COMMUNICATION

View Article Online
View Journal | View Issue

Cite this: *Chem. Commun.*, 2019, 55, 632

Received 31st August 2018,
Accepted 10th December 2018

DOI: 10.1039/c8cc07076h

rsc.li/chemcomm

Solvent-free lithium and sodium containing electrolytes based on pseudo-delocalized anions†

Juan Forero-Saboya, ‡[a] Elham Hosseini-Bab-Anari, ‡[b] Muhammad E. Abdelhamid, [a] Kasper Moth-Poulsen [b] and Patrik Johansson *[ac]

Mixing the standard battery salt LiTFSI with various Li-salts of novel pseudo-delocalized organic anions $[N(CH_3)_2((CH_2)_nSO_3)((CH_2)_mSO_3)]^-$ (MM_{nm11}), results in super-cooled solvent-free liquid electrolytes with glass transition temperatures of *ca.* 50 °C. Synthesis routes and full chemical characterisation of the new pseudo-delocalized anions are presented, as well as phase and thermal stabilities. The ion conductivities and electrochemical stabilities are evaluated towards lithium and sodium battery application.

Conventional lithium-ion battery (LIB) electrolytes are composed of lithium salts with weakly coordinating anions, such as hexafluorophosphate[1] (PF_6^-), tetrafluoroborate[2] (BF_4^-), bis(oxalate)borate[3] (BOB), or bis(trifluoromethanesulfonyl)-imide[4] (TFSI), dissolved in a mixture of organic solvents (often linear and cyclic carbonates) at *ca.* 1 M concentrations.[5,6] Their wide electrochemical stability windows (ESWs) allow the use of high voltage positive electrodes, such as $LiCoO_2$ (4 V *vs.* Li^+/Li), and graphite negative electrodes (0.1 V *vs.* Li^+/Li), by virtue of the creation of a solid electrolyte interphase (SEI). This, together with the large capacities of the electrodes, enable a very high specific energy. But the safety of LIBs remains a major concern mainly due to the highly flammable organic solvents used.

The combination of ever higher energy densities and voltages of the cells with the highly flammable organic solvents[7] directs particular attention towards creating novel electrolytes with improved safety characteristics. For example, replacing the organic solvents by an ionic liquid matrix improves the thermal stability drastically and decreases the flammability,[8] but at the same time, both the lithium transference number and the electrolyte fluidity often decreases, thus reducing the electrochemical performance.

All solid-state batteries (ASSBs),[9,10] in which the conventional electrolytes have been replaced by a solid-state electrolyte (SSE), also claim to provide remarkable safety characteristics. However, most SSEs suffer from low room temperature ionic conductivities, often three orders of magnitude lower than liquid electrolytes, hence they usually operate at elevated temperatures (*ca.* 80 °C),[11] even if there exist polymer electrolytes with acceptable ionic conductivities at room temperature (1 mS cm^{-1}). As a result, however, the concept of high-temperature lithium-ion batteries (HT-LIB) has emerged.[12]

Another alternative is "thermal" batteries, operating between 350 °C and 550 °C and employing molten salt mixtures as liquid solvent-free electrolytes, with high thermal stability, low flammability, and high ionic conductivity.[11] In order to utilize this concept for LIBs, the melting temperature must decrease significantly – but even if these electrolytes do not reach the conductivities needed at room temperature, they might be applied in HT-LIBs. This has been achieved by combining two or three alkali cation salts with a common weakly coordinating anion, such as TFSI,[13,14] bis(fluorosulfonyl)imide (FSI),[15] or triflate.[16] Such eutectic mixtures have promising ionic conductivities and form stable SEIs on typical LIB electrode materials. The molar fraction of Li^+ is, however, quite low, which severely limits the rate capability of the cells despite the elevated operating temperature.[17] Additionally, the presence of other alkali metal cations may interfere with the electrochemistry by unwanted plating or co-intercalation. The approach has its origin in enhanced ion conductivities by the "mixed alkali effect" of glassy and polymeric electrolytes, explored for batteries in the early 1990's.[18,19]

Herein, an alternative strategy is explored to create solvent-free electrolytes; mono-cationic–di-anionic mixtures, *i.e.* mixing two Li-salts with different anions, using the unique design of three different pseudo-delocalized (*i.e.* the negative charge

[a] *Department of Physics, Chalmers University of Technology, SE-412 96 Gothenburg, Sweden. E-mail: patrik.johansson@chalmers.se*
[b] *Department of Chemistry and Chemical Engineering, Chalmers University of Technology, SE-412 96 Gothenburg, Sweden*
[c] *ALISTORE – European Research Institute, CNRS FR 3104, Hub de l'Energie, Rue Baudelocque, 80039 Amiens Cedex, France*

† Electronic supplementary information (ESI) available: Experimental procedure, synthesis of the MM_{nm11} salts, NMR spectra and additional figures and tables. See DOI: 10.1039/c8cc07076h

‡ These authors have contributed equally to this work.

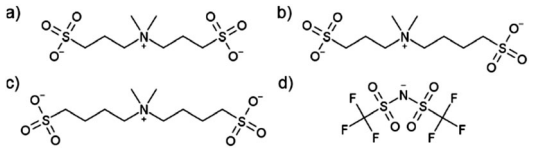

Fig. 1 Chemical structures of the anions employed: (a) MM_{3311}: 3,3′-(dimethylammonio)bis(propane-1-sulfonate), (b) MM_{3411}: 4-(dimethyl(3-sulfonatopropyl)ammonio)butane-1-sulfonate, (c) MM_{4411}: 4,4′-(dimethylammonio)bis(butane-1-sulfonate), and (d) TFSI: bis(trifluoromethylsulfonyl)imide.

delocalized by being localized at several central in the structure) anions $[N(CH_3)_2((CH_2)_nSO_3)((CH_2)_mSO_3)]^-$ (MM_{nm11}, Fig. 1)[20,21] – aiming primarily at HT-LIB application. We explore the previously reported lithium and sodium salts of MM_{4411} together with a new symmetric anion (MM_{3311}) as well as an asymmetric anion (MM_{3411}), all synthesized with high purity and excellent yield in three consecutive steps from readily available pre-cursors with minimal usage of solvent on multiple gram scale, expected to be scaled-up to kg scale without any practical difficulties. An electrolyte based 100% on salts is likely to initially be more expensive than a 1 M Li-salt liquid electrolyte, but improved battery safety and life-length may result. The here presented anions are likely to be cheap to produce based on the pre-cursors. The synthesis details and the full characterisation is found in the ESI.†

First, the thermal stabilities of the MM_{nm11} salts were assessed, whereafter their mixtures with TFSI salts were explored by constructing a series of quasi-phase diagrams highlighting the glass transition temperatures (T_gs) and melting points. Second, the ion conductivities as a function of both temperature and composition were studied and analysed using free volume theory. Finally, the lithium-only composition with the lowest T_g was selected for proof-of-concept electrochemical stability tests aiming towards lithium battery application.

The pure salts $LiMM_{3311}$ and $LiMM_{3411}$ exhibit very similar thermal behaviour. The first weight loss of ~1.8% at 140 °C is most likely due to residual water from the synthesis (Fig. 2a) as confirmed by TGA-FTIR evolved gas analysis (Fig. 2b), where the mass loss clearly observed in the derivate of the thermogravimetric signal (dTG) corresponds to an increased H_2O bend band signal. Both salts decompose at *ca.* 280 °C, as observed in the dTG signal and an increased C–H stretching band intensity.

In stark contrast the $LiMM_{4411}$ salt decomposes much later, at *ca.* 350 °C, implying higher stability of butylsulfonate side chains. We can only speculate the reason for this to be the formation of a more stable transition state during the decomposition reaction by the creation of six-membered rings. Several mixtures of LiTFSI and $LiMM_{nm11}$ salts were prepared in order to obtain low melting temperature eutectics, and compared to LiTFSI (m.p. 234 °C), the melting points decrease as expected.[22]

In all systems, the formation of an amorphous phase was observed (Fig. 3) and above 20–30 mol% of $LiMM_{nm11}$ the systems were fully amorphous. These systems are very phase-stable with no crystallization detectable even after three months, while for 40–50 mol% of $LiMM_{3311}$ the systems crystallize, likely driven by anion stacking (Fig. S12, ESI†).

Obtaining glassy solids simply by solvent evaporation is surprising as it most often results in salt precipitation as the concentration increases. In contrast, we observe here a rapid increase in viscosity of the liquids during drying, which causes the activation energy for fluid flow to exceed the energy gain either by crystal formation or growth.[23] Although this mechanism is often found for quenched salt melts, we believe it applies here when our mixtures lose water. This also explains the increase in the glass transition temperature for the compositions with more MM_{nm11} anion content, as their aqueous solutions have higher viscosities and lose fluidity at higher temperatures.

The abrupt increase in viscosity prevents the mixtures to get fully dry by hindering the diffusion of water, resulting in residual water content of 0.1–0.2 wt%, ≫ the *ca.* 100 ppm reported for other solvent-free electrolytes. This is, however, expected to have little/no effect on the electrochemistry given its low mobility and activity, as has recently been established for water-in-salt electrolytes with much higher water contents.[24]

By mixing LiTFSI with the $LiMM_{nm11}$ salts significantly decreased melting points were achieved, but the glass transition temperatures are still above 50 °C. This renders them too viscous for battery application, even for HT-LIBs. In order to further decrease the glass transition temperatures and the viscosities, a series of quaternary systems, *i.e.* $Li_{1-x}Na_x(TFSI)_{1-y}(MM_{nm11})_y$ were made, making use of the larger and therefore less polarising, and

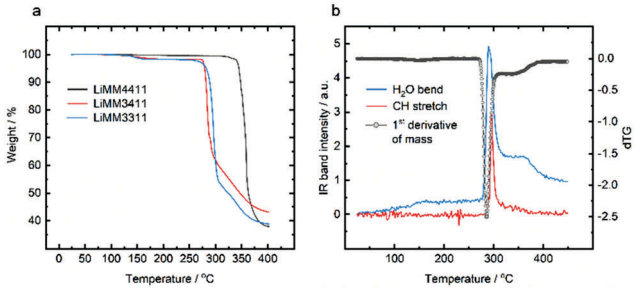

Fig. 2 (a) TGA traces of the $LiMM_{nm11}$ salts (the corresponding $NaMM_{nm11}$ salts present similar behaviour (Fig. S11, ESI†)), (b) FTIR band intensities evolution with temperature for the thermal analysis of $LiMM_{3411}$, and (c) first derivative of the TGA signal of $LiMM_{3411}$.

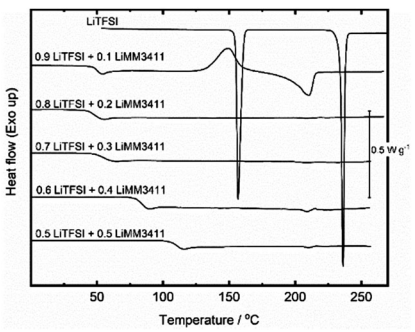

Fig. 3 DSC traces of the LiTFSI–$LiMM_{3411}$ systems with compositions in molar fractions.

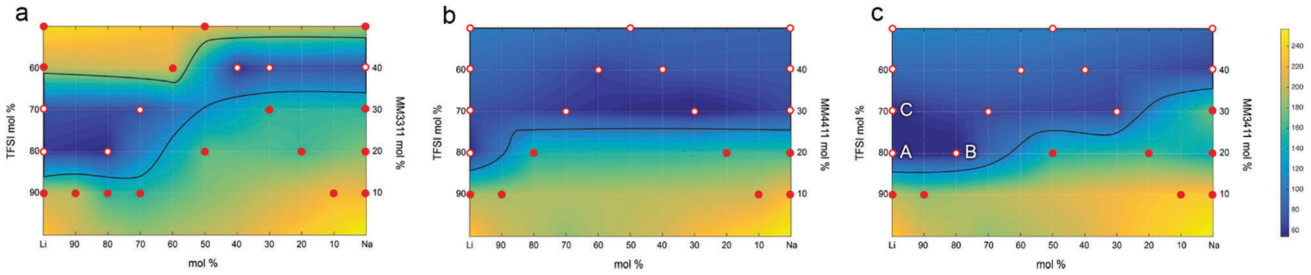

Fig. 4 Quasi-phase diagram for the quaternary mixtures containing MM_{3311}, MM_{4411}, and MM_{3411}. The colours are only for visual aid. The bullets represent data points, hollow mark totally amorphous compositions. Values for $Li_xNa_{1-x}TFSI$ are from the literature.[14]

less coordinating Na^+ cation.[25] From DSC data, three quasi-phase diagrams were created for TFSI contents above 50 mol% (Fig. 4). These mixed anion-mixed cation systems have composition areas where no crystalline phases were observed. In the fully amorphous regions (blue), the partial substitution of Li by Na decreased the glass transition temperatures slightly (*e.g.* A to B in Fig. 4c). This effect was limited up to 20–30 mol% of Na^+, where it favours the formation of crystalline phases above these concentrations. The trend observed for the binary systems extends to any cation composition and increasing the MM_{nm11} content (*e.g.* A to C in Fig. 4c) produces a corresponding increase in T_g. The ionic conductivities of $Li(TFSI)_{0.8}(MM_{3411})_{0.2}$, $Li_{0.8}Na_{0.2}(TFSI)_{0.8}(MM_{3411})_{0.2}$ and $Li(TFSI)_{0.7}(MM_{3411})_{0.3}$ all follow the same trend; cation substitution (Li to Na) produces only a two-fold increase, while anion substitution a two order of magnitude increase (Fig. 5a) – the latter is related to the $\sim$10 °C decrease in T_g as 10 mol% of the anion was substituted. The effect is less evident at higher temperatures as the free volume increases and allows all ions to migrate.

The T_gs obtained from the DSC traces agree with the overall changes in the conductivities observed in the Arrhenius plots; above T_g the ionic conductivity follows the Vogel–Fulcher–Tamman (VFT) relation:

$$\ln\left(\sigma_0 T^{1/2}\right) = \ln A - {}^{E}/_{k_B}(T - T_0) \qquad (1)$$

where σ_0 is the ionic conductivity at temperature T (in K), k_B is the Boltzmann constant, the parameters A and T_0 are fitting constants and E is the pseudo-activation energy for viscous flow.[26] The Vogel temperature (T_0) is related to the point when the free volume in the structure disappears.[27,28] For the mixtures based on MM_{3411}, slightly lower T_0 are obtained than for the MM_{3311} and MM_{4411} based mixtures (Table S2, ESI†). This might be related to the difficulty of forming organized structures by asymmetric anions, providing lower viscosity and higher conductivity (Fig. 5b). The way the different ions interact and organize themselves at temperatures above T_g affects their mobility, which is roughly inversely proportional to their ionic radii.[29] Hence, the large MM_{nm11} and TFSI anions are very unlikely to find accessible free volume of suitable size in their local environment, rendering them largely immobile. The lithium cation transference number is therefore expected to approach unity, but the total ion conductivities are still 1–2 orders of magnitude lower than other types of single-ion conductors, such as some block copolymers[30] or crystalline LISICON-type electrolytes.[9] The main difference from our single-ion conductor systems is the fact that they are liquids at moderate temperatures (*ca.* 60 °C) and therefore they are difficult to compare directly.

Kubota and Matsumoto[31] reported on a more closely related system, with a bulky anion similar to TFSI operating at 150 °C, resulting in a very high Li^+ transference number of 0.94. Compared to the system of Kubota (10^{-2} S cm^{-1} at 100 °C), the rather low conductivities observed here are likely due to the higher viscosities from our larger anions and a higher degree of ion association.[32] Speculatively the sulfonate groups of the MM_{nm11} anions might act as Li^+ traps[20] and promote the formation of large aggregates (Fig. 6). The local structure was unfortunately not possible to be unambiguously resolved by *e.g.* IR or Raman spectroscopy (not shown). The partial substitution of Li^+ by Na^+ perturbs the aggregate structure, creates free volume, and increase the ion conductivity (Fig. 5).

The atomic fraction of the cation of interest (Li^+ or Na^+), which would have an influence on the C-rate capability, is *ca.* 5% (excl. H), close to the 8% for the system of Kubota. In comparison, polymeric single-ion conductors (SICs), with the same ion conduction mechanism, are often at *ca.* 1%, while

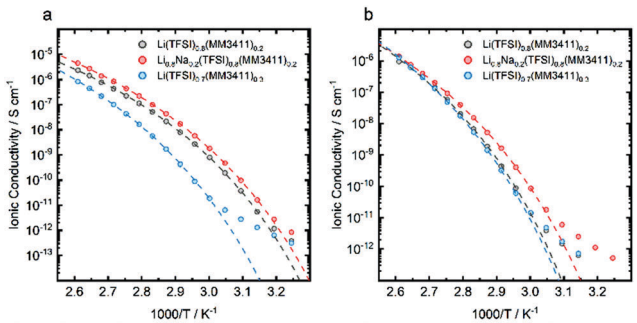

Fig. 5 Arrhenius plot of the ionic conductivities of (a) $Li(TFSI)_{0.8}(MM_{3411})_{0.2}$, $Li_{0.8}Na_{0.2}(TFSI)_{0.8}(MM_{3411})_{0.2}$ and $Li(TFSI)_{0.7}(MM_{3411})_{0.3}$, and (b) for mixtures with different MM_{nm11} anions.

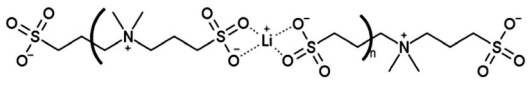

Fig. 6 Schematic of possible aggregate structures.

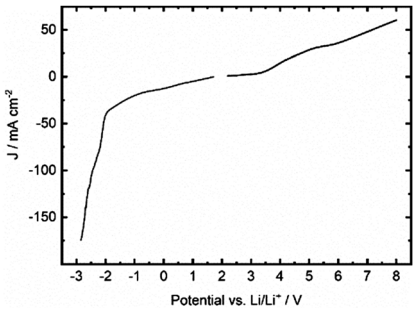

Fig. 7 Cathodic and anodic LSV traces for $Li(TFSI)_{0.8}(MM_{3411})_{0.2}$.

crystalline LISICON is at *ca.* 40%, but the conduction mechanism differs significantly.

From the above, $Li(TFSI)_{0.8}(MM_{3411})_{0.2}$ was selected for proof-of-concept of electrochemical stability tests. In the anodic part of the LSV, a two-step decomposition is observed (Fig. 7). The first step at 3.5 V *vs.* Li^+/Li is attributed to the decomposition of MM_{3411}, expected to have a lower oxidation potential than TFSI,[20] while the second step, above 5 V *vs.* Li^+/Li likely corresponds to TFSI decomposition.[33] Both steps are hard to resolve in the voltammogram as the current responses overlap. This can be attributed to the high electrolyte viscosity, resulting in slow diffusion of MM-anion decomposition by-products away from the electrode surface. The ''tail'' in the trace corresponds to a constant anion decomposition at the electrode surface. As compared to liquid LIB electrolytes a reduced slope is observed, simply an effect of viscosity induced mass transfer limitations.

On the cathodic side, due to the low electrolyte conductivity, the small peak at *ca.* 0 V *vs.* Li/Li^+ is truly believed to correspond to minor lithium ion reduction and lithium metal plating, while the large feature below −2 V *vs.* Li/Li^+ is due to TFSI anion reduction and decomposition. This very low cathodic limit differs significantly from the reduction potential previously predicted for TFSI,[34] likely due to a large polarization build up between working and counter electrodes in the experimental set-up.

In conclusion, high purity and yield synthesis and full characterization of new Li/Na salts based on pseudo-delocalized anions (MM_{nm11}) was reported. Different combinations with LiTFSI were investigated as prospective battery electrolytes. The presence of 20–30 mol% of the MM_{nm11} anions prevents completely crystallization, which proves the possible preparation at moderate temperatures (*ca.* 60 °C) of a liquid completely solvent-free electrolytes. The effect is more evident for the asymmetric MM_{3411} anion as organized packing is further inhibited and opens for further exploring alternative flexible and bulky anions to form solvent-free battery electrolytes. Additionally, the presence of the bulky pseudo-delocalized MM_{nm11} anions seems to have a positive effect on the Li^+ transference number. Apart from using the asymmetry of the MM_{nm11} anions the ionic conductivity might be improved by reducing the ion–ion interaction further by replacing the $-SO_3^-$ moieties by more weakly cation coordinating units *e.g.* $-SO_2-N^--SO_2CF_3$, as already shown effective in block co-polymer SICs.[30]

We are grateful for the support by Chalmers, the Erasmus Mundus joint master program; Materials for Energy Storage and Conversion (M.E.S.C.) (JFS) and the financial support by the Swedish Energy Agency (''Batterifonden'' grants #37671-1 & #37685-1), as well as Chalmers Battery Initiative and Areas of Advance; Energy, Materials Science, and Transport.

Conflicts of interest

There are no conflicts to declare.

Notes and references

1 K. Ozawa, *Solid State Ionics*, 1994, **69**, 212–221.
2 Y. Matsuda, M. Morita and T. Yamashita, *J. Electrochem. Soc.*, 1984, **131**, 2821–2827.
3 K. Xu, *J. Electrochem. Soc.*, 2008, **155**, A733.
4 M. Montanino, S. Passerini and G. B. Appetecchi, *Rechargeable Lithium Batteries: From Fundamentals to Applications*, Woodhead Publishing, 2015, pp. 73–116.
5 K. Xu, *Chem. Rev.*, 2004, **104**, 4303–4418.
6 J. Wen, Y. Yu and C. Chen, *Mater. Express*, 2012, **2**, 197–212.
7 A. Balducci, *Top. Curr. Chem.*, 2017, **375**, 20.
8 E. Quartarone and P. Mustarelli, *Chem. Soc. Rev.*, 2011, **40**, 2525–2540.
9 J. G. Kim, B. Son, S. Mukherjee, N. Schuppert, A. Bates, O. Kwon, M. J. Choi, H. Y. Chung and S. Park, *J. Power Sources*, 2015, **282**, 299–322.
10 L. Long, S. Wang, M. Xiao and Y. Meng, *J. Mater. Chem. A*, 2016, **4**, 10038–10069.
11 N. Plylahan, M. Kerner, D.-H. Lim, A. Matic and P. Johansson, *Electrochim. Acta*, 2016, **216**, 24–34.
12 R. A. Guidotti and P. Masset, *J. Power Sources*, 2006, **161**, 1443–1449.
13 K. Kubota, T. Nohira, T. Goto and R. Hagiwara, *J. Chem. Eng. Data*, 2008, **53**, 2144–2147.
14 R. Hagiwara, K. Tamaki, K. Kubota, T. Goto and T. Nohira, *J. Chem. Eng. Data*, 2008, **53**, 355–358.
15 F. Xu, C. Liu, W. Feng, J. Nie, H. Li, X. Huang and Z. Zhou, *Electrochim. Acta*, 2014, **135**, 217–223.
16 X. Tu, Y. Chu and C. Ma, *Ionics*, 2010, **16**, 81–84.
17 A. Watarai, K. Kubota, M. Yamagata, T. Goto, T. Nohira, R. Hagiwara, K. Ui and N. Kumagai, *J. Power Sources*, 2008, **183**, 724–729.
18 J. O. Isard, *J. Non-Cryst. Solids*, 1969, **1**, 235–261.
19 B. Chowdari, R. Huq and G. Farrington, *Solid State Ionics*, 1992, **57**, 49–58.
20 E. Jónsson, M. Armand and P. Johansson, *Phys. Chem. Chem. Phys.*, 2012, **14**, 6021.
21 E. Hosseini-Bab-Anari, A. Boschin, T. Mandai, H. Masu, K. Moth-Poulsen and P. Johansson, *RSC Adv.*, 2016, **6**, 85194–85201.
22 M. Hillert, *Phase Equilibria, Phase Diagrams and Phase Transformations*, Cambridge University Press, Cambridge, 2nd edn, 2008.
23 D. Turnbull and M. H. Cohen, *J. Chem. Phys.*, 1958, **29**, 1049–1054.
24 M. S. Ding, A. Von Cresce and K. Xu, *J. Phys. Chem. C*, 2017, **121**, 2149–2153.
25 A. Ponrouch, D. Monti, A. Boschin, B. Steen, P. Johansson and M. R. Palacín, *J. Mater. Chem. A*, 2015, **3**, 22–42.
26 D. Bamford, A. Reiche, G. Dlubek, F. Alloin, J.-Y. Sanchez and M. A. Alam, *J. Chem. Phys.*, 2003, **118**, 9420–9432.
27 G. Dlubek, Y. Yu, R. Krause-Rehberg, W. Beichel, S. Bulut, N. Pogodina, I. Krossing and C. Friedrich, *J. Chem. Phys.*, 2010, **133**, 124502.
28 L. S. García-Colín, L. F. del Castillo and P. Goldstein, *Phys. Rev. B: Condens. Matter Mater. Phys.*, 1989, **40**, 7040–7044.
29 A. P. Abbott, *ChemPhysChem*, 2005, **6**, 2502–2505.
30 R. Bouchet, *et al.*, *Nat. Mater.*, 2013, **12**, 452–457.
31 K. Kubota and H. Matsumoto, *J. Phys. Chem. C*, 2013, **117**, 18829–18836.
32 D. R. MacFarlane, M. Forsyth, E. I. Izgorodina, A. P. Abbott, G. Annat and K. Fraser, *Phys. Chem. Chem. Phys.*, 2009, **11**, 4962.
33 M. Ue, M. Takehara, S. Mori and M. C. Corporation, *J. Electrochem. Soc.*, 1997, **144**, 2684–2688.
34 L. Suo, O. Borodin, T. Gao, M. Olguin, J. Ho, X. Fan, C. Luo, C. Wang and K. Xu, *Science*, 2015, **350**, 938–943.